



Hypoxia-inducible factor 1 α enhances RANKL-induced osteoclast differentiation by upregulating the MAPK pathway

Dong Wang^{1,2#}, Lin Liu^{1#}, Zechao Qu^{1,2}, Bo Zhang^{1,2}, Xiangcheng Gao^{1,2}, Wangli Huang^{1,2}, Mingzhe Feng^{1,2}, Yining Gong¹, Lingbo Kong¹, Yanjun Wang¹, Liang Yan¹

¹Department of Orthopedic Surgery, Xi'an Honghui Hospital, Xi'an Jiaotong University, School of Medicine, Xi'an, China; ²School of Medicine, Yanan University, Yanan, China

Contributions: (I) Conception and design: D Wang, L Liu, L Yan, Y Wang, L Kong, Z Qu; (II) Administrative support: D Wang, L Yan; (III) Provision of study materials or patients: L Kong, L Yan; (IV) Collection and assembly of data: B Zhang, M Feng, X Gao, W Huang, Y Gong; (V) Data analysis and interpretation: All authors; (VI) Manuscript writing: All authors; (VII) Final approval of manuscript: All authors.

[#]These authors contributed equally to this work.

Correspondence to: Liang Yan; Yanjun Wang. Xi'an Honghui Hospital, Xi'an Jiaotong University, School of Medicine, Xi'an 710000, China. Email: yanliangdr5583@163.com; thomaswyj@163.com.

Background: Hypoxia (low-oxygen tension) and excessive osteoclast activation are common conditions in many bone loss diseases, such as osteoporosis, rheumatoid arthritis (RA), and pathologic fractures. Hypoxia-inducible factor 1 alpha (HIF1 α) regulates cellular responses to hypoxic conditions. However, it is not yet known how HIF1 α directly affects osteoclast differentiation and activation. This study sought to explore the effects of HIF1 α on osteoclast differentiation and its molecular mechanisms.

Methods: L-mimosine, a prolyl hydroxylase (PHDs) domain inhibitor, was used to stabilize HIF1 α in normoxia. In the presence of receptor activator of nuclear factor- κ B (NF- κ B) ligand (RANKL), RAW264.7 cells were cultured and stimulated by treatment with L-mimosine at several doses to maintain various levels of intracellular HIF1 α . The multi-nucleated cells were assessed by a tartrate-resistant acid phosphatase (TRAP) and F-actin ring staining assays. The osteoclast-specific genes, such as Cathepsin K, β 3-Integrin, TRAP, c-Fos, nuclear factor of activated T cells, cytoplasmic 1 (NFATc1), and matrix metallo-proteinase 9 (MMP9), were analyzed by real time-polymerase chain reaction (RT-PCR). The expression of relevant proteins was analyzed by Western blot.

Results: L-mimosine increased the content of intracellular HIF1 α in a dose-dependent manner, which in turn promoted RANKL-induced osteoclast formation and relevant protein expression by upregulating the mitogen-activated protein kinase (MAPK) pathways.

Conclusions: Our findings suggest that HIF1 α directly increases the osteoclast differentiation of RANKL-mediated RAW264.7 cells *in vitro* by upregulating the MAPK pathways.

Keywords: Hypoxia-inducible factor 1 alpha (HIF1 α); L-mimosine; osteoclast; RAW264.7 cells; mitogen-activated protein kinase pathway (MAPK pathway)

Submitted Sep 02, 2022. Accepted for publication Oct 21, 2022.

doi: 10.21037/atm-22-4603

View this article at: <https://dx.doi.org/10.21037/atm-22-4603>

Introduction

The bone is a hard organ composed of calcium salts that support the tissues of the body. Contrary to previous understandings, the bones continue to undergo highly dynamic reconstruction to maintain their structure

and function (1,2). The main cells involved in bone reconstruction include osteoclasts, which absorb damaged bones (3), and osteoblasts, which build new bones (4). Osteoclasts are unique multi-nucleated giant cells formed from bone marrow hematopoietic stem cells through the

synergistic action of multiple systemic hormones and cytokines (1). Enhanced osteoclast differentiation and functional activities are the major causes of bone diseases, such as osteoporosis, rheumatoid arthritis (RA), and pathologic fractures (5), and hypoxia is a common feature of these diseases (6).

The RANKL is a major osteoclastogenic molecule (7). RAW264.7 cells are often regarded as suitable progenitors for inducing osteoclasts, and can be transformed into osteoclasts by treatment with RANKL makes it easier for researchers to study osteoclasts (8). The binding of RANKL and its receptor (RANK) activates tumor necrosis factor receptor-associated factor 6 (TRAF6) (9), nuclear factor-kappa B (NF- κ B), and mitogen-activated protein kinases (MAPKs), including extracellular signal-regulated kinase 1/2 (ERK1/2), p38, and stress-activated protein kinase/c-Jun N-terminal kinase (SAPK/JNK) (10-12), and induces c-Fos, c-Jun, and the nuclear factor of activated T cells, cytoplasmic 1 (NFATc1) (13-15). These cytokines stimulate osteoclast differentiation by regulating the expression of osteoclast-related genes, including tartrate-resistant acid phosphatase (TRAP) (16), cathepsin K, matrix metalloproteinase 9 (MMP9), and β 3-Integrin (17).

Hypoxia-inducible factor (HIF) is a major transcription factor that induces cellular responses to hypoxic conditions (18). It is composed of a subunit regulated by the oxygen content [i.e., hypoxia-induced factor 1 α (HIF1 α)], and a subunit of sustained expression [i.e., hypoxia-induced factor 1 beta (HIF1 β)], which play pivotal roles in bone formation (19-22). Other studies have shown that MAPKs and HIF1 α influence each other (23-25); however, the effect of HIF1 α on MAPKs in regulating osteoclast differentiation and activation is unknown. Prolyl hydroxylases (PHDs) act as cellular oxygen sensors (26), and HIF1 α is degraded by PHDs under normoxia (27-29). L-mimosine, which is a PHD inhibitor, can be used to increase HIF1 α expression in research (30,31).

The current studies mainly focused on the effect of hypoxia on the microenvironment which osteoclast survived in rather than exploring the direct effects on osteoclast differentiation. In our study, we hypothesized that L-mimosine-induced HIF1 α would directly promote osteoclast differentiation. Evidence that L-mimosine-induced HIF1 α directly promotes osteoclast differentiation will provide novel ideas and directions for research on the treatment of bone loss diseases. We present the following article in accordance with the MDAR reporting checklist (available at <https://atm.amegroups.com/article/>

[view/10.21037/atm-22-4603/rc](https://doi.org/10.21037/atm-22-4603/rc)).

Methods

Media, reagents, and antibodies

L-mimosine (>98% purity; see *Figure 1A*) was obtained from Sigma-Aldrich (St Louis, MO, USA) and dissolved in 50 mg/mL of 1 M NH₄OH (31). BAY-87-2243 (a HIF1 α -specific inhibitor; see *Figure 1B*) was provided by Sigma-Aldrich (St Louis, MO, USA) and dissolved in 2 mg/mL of dimethyl sulfoxide (32). Fetal bovine serum (FBS), alpha modified Eagle's medium (α -MEM), and Dulbecco's modified Eagle's medium (DMEM) were purchased from Gibco (Rockville, MD, USA). Soluble recombinant RANKL was obtained from PeproTech (Rocky Hill, NJ, USA). The TRAP kit was purchased from Sigma-Aldrich (St Louis, MO, USA). Primary antibodies for c-Fos and NFATc1 were purchased from Abcam (USA), and c-Jun, phosphor-ERK, ERK, phosphor-p38, p38, phosphor-JNK, JNK, β -actin, and HIF1 α were purchased from Beyotime (Shanghai, China).

Cell cultures

The RAW264.7 cell lines were obtained from the American Type Culture Collection (ATCC, Manassas, VA, USA), maintained in complete DMEM (a high glucose medium) with 10% FBS at 37 °C in a 5% carbon dioxide atmosphere and 95% humidity. The RAW264.7 cells were passaged, and induction started from passages 10-15 after reaching 70-80% density. To generate osteoclasts, RAW264.7 cells (2×10^3 cells/well) were seeded into a 96-well-plate with the DMEM for 12 h, after which the DMEM was discarded and the cells were further cultured in an induction media (α -MEM) in the presence of 35 ng/mL RANKL and different doses of L-mimosine at 50, 100, and 150 μ M for 5 days.

Cytotoxicity assays

To evaluate the effects of L-mimosine and BAY-87-2243 on the activities of the RAW264.7 cells, the cells were seeded into 96-well plates at a density of 2×10^3 cells/well and left overnight. Different concentrations of L-mimosine were fixed at 0, 50, 100, 150, and 200 μ M (22). Similarly, BAY-87-2243 was added at various concentrations (0, 5, 10, 20, and 40 nM). After 48 h, 10 μ L of Cell Counting Kit-8 (CCK-8) solution (KeyGen Biotech, Nanjing, China) was

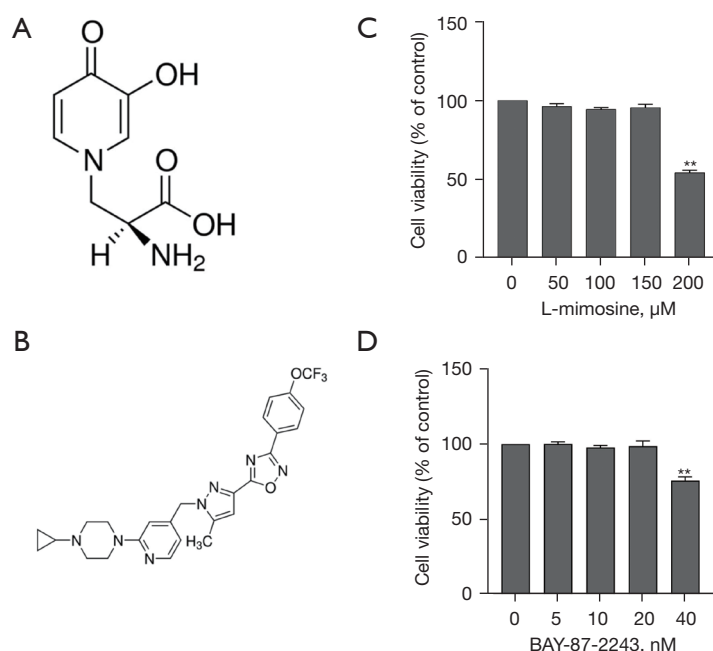


Figure 1 L-mimosine and BAY-87-2243 exerts no cytotoxicity at the experimental concentrations. (A) The chemical structure of L-MIM. (B) The chemical structure of BAY-87-2243. The RAW264.7 cells were treated with different concentrations of (C) L-mimosine (0, 50, 100, 150, and 200 μM) and (D) BAY-87-2243 (0, 5, 10, 20, and 40 nM) for 2 days. Cell viability was measured by CCK-8 assays. The data are expressed as the mean \pm SD of the 3 independent experiments; **, $P < 0.01$ vs. control group. L-MIM, L-mimosine; CCK-8, Cell Counting Kit-8.

added, and cytotoxicity assays were performed using the CCK-8 in accordance with the manufacturer's instructions. The absorbance at 450 nm was measured using a microplate reader (Thermo Electron Corp., Waltham, MA, USA).

TRAP staining

After osteoclast differentiation, the cells were washed with phosphate-buffered saline (PBS), fixed with 4% paraformaldehyde for 10 min, and stained for TRAP using a leukocyte acid phosphatase cytochemistry kit (Sigma-Aldrich, St Louis, MO, USA) in accordance with the manufacturer's instructions. TRAP-positive multi-nucleated cells containing 3 or more nuclei were marked as osteoclasts under a light microscope (OLYMPUS, Japan).

F-actin ring staining

After washing 3 times with PBS, the cells were fixed with 4% paraformaldehyde, and the cells were then washed 3 more times with PBS before permeabilization with 0.1% Triton X-100 and incubation with Alexa Fluor 488-phalloidin

(Thermo Fisher Scientific, USA) for 60 min. After washing with PBS, the cells were incubated with 4',6-diamidino-2-phenylindole (Roche, Basel, Switzerland) for 10 min and photographed under a fluorescence microscope.

Western blot analysis

The RAW264.7 cells were seeded in a 6-well plate at a density of 2×10^6 cells/well and incubated for 12 h. Similar to the induction of the osteoclasts, the culture medium was changed to induction media with or without different concentrations of L-mimosine to induce HIF1 α for 30 min before stimulating with 35 ng/mL of RANKL. To inhibit HIF1 α expression, BAY-87-2243 was added to another group that already contained L-mimosine and RANKL. The proteins were extracted from the samples using radioimmunoprecipitation buffer (Sigma-Aldrich St Louis, MO, USA) with protease and phosphatase inhibitors and normalized to determine protein concentrations using the bicinchoninic acid method. Equal amounts of protein were loaded onto 10% sodium dodecyl sulfate-polyacrylamide gel electrophoresis gels and electro-transferred to polyvinylidene

Table 1 The primer pairs used in this study

Gene	Primer forward	Primer reverse
<i>c-Fos</i>	5'-CGACCATGATGTTCTCGGGT-3'	5'-TCGGCTGGGGAATGGTAGTA-3'
<i>NFATc1</i>	5'-AGGACCCGGAGTTCGACTT-3'	5'-AGGTGACACTAGGGGACACA-3'
<i>TRAP</i>	5'-TGTCCGCTTGAGGGTACATT-3'	5'-GCAGGACAGCCCTTAGCATC-3'
<i>MMP9</i>	5'-CCAGCCGACTTTTGTGGTCT-3'	5'-CTTCTCTCCCATCATCTGGGC-3'
<i>cathepsin K</i>	5'-CTGGAGGGCCAACCTCAAGAA-3'	5'-TGGCCACATATGGGTAAGC-3'

difluoride membranes (Bio-Rad, Hercules, CA, USA). After blocking in 5% non-fat milk for 1 h, appropriately diluted primary antibodies were added, and the membranes were incubated at 4 °C overnight. Next, the membranes were washed and incubated with horseradish peroxidase-conjugated secondary antibody for 2 h at room temperature and detected using enhanced chemiluminescence. Finally, densitometric values were quantified for each band using ImageJ software (version 1.53 K).

RNA extraction and quantitative real-time polymerase chain reaction (qRT-PCR)

The RAW264.7 cells were inoculated into a 6-well plate, as described preceding part of the text, in the presence of RANKL (35 ng/mL) and treated with or without L-mimosine and BAY-87-2243 for 24 h. Total RNA was isolated from the cells using TRIzol reagent (Thermo Fisher Scientific, USA) in accordance with the manufacturer's instructions. Complementary deoxyribonucleic acid was synthesized using a reverse transcriptase kit (Takara Biotechnology, Japan) and used as a template for qRT-PCR with SYBR® Premix Ex Taq™ II (Takara, Japan). The following primers were showed in *Table 1*. The conditions for the PCR amplification reaction were: 95 °C for 30 s, 95 °C for 5 s, and 60 °C for 34 s, which was repeated for a total of 40 cycles. β -Actin was used as an internal control.

Statistical analysis

All the data are expressed as the mean \pm standard deviation (SD). The statistical analysis was performed using SPSS software package version 18.0 and GraphPad Prism 8.0 (GraphPad Software, San Diego, CA, USA). Statistical differences between groups were calculated and analyzed using a 1-way analysis of variance with Tukey's test, and statistical significance was set at $P < 0.05$.

Results

L-mimosine increases the HIF1 α expression in RAW264.7 cells

The cytotoxicity assays revealed that only high concentrations of L-mimosine (200 μ M; see *Figure 1C*) and BAY-87-2243 (40 nM; see *Figure 1D*) exerted a cytotoxic effect on the RAW264.7 cells. HIF1 α expression in the RAW264.7 cells cultured with RANKL (35 ng/mL) with or without L-mimosine (50, 100, or 150 μ M) was analyzed using western blot assays, and the results showed that HIF1 α expression was positively correlated with L-mimosine concentration (see *Figure 2A,2B*). Additionally, in another RAW264.7 group, the cells treated with the specific inhibitor of HIF1 α (BAY-87-2243) (10 nM) reversed the induction effect of L-mimosine on HIF1 α expression (see *Figure 2C,2D*).

HIF1 α facilitates RANKL-induced osteoclast differentiation and F-actin ring formation

To exclude the possible effects of L-mimosine on cell viability, osteoclasts were induced from the RAW264.7 cells by RANKL (35 ng/mL) to validate the HIF1 α effects in the osteoclastogenesis. TRAP staining is considered a common and reliable way to identify osteoclasts; the cells can be treated as osteoclasts when TRAP staining is positive, and the nuclear number is ≥ 3 . On day 5, the control group cultured with RANKL differentiated into mature TRAP-positive multi-nucleated cells (red), and cell differentiation increased in a dose-dependent manner, which was stimulated by L-mimosine (see *Figure 3A,3B*). However, osteoclastogenesis enhancement was eliminated by the addition of BAY-87-2243 (see *Figure 3C,3D*). The F-actin ring is critical for mature osteoclasts to achieve bone resorption. Using rhodamine-phalloidin staining, our results revealed that HIF1 α , which was induced by

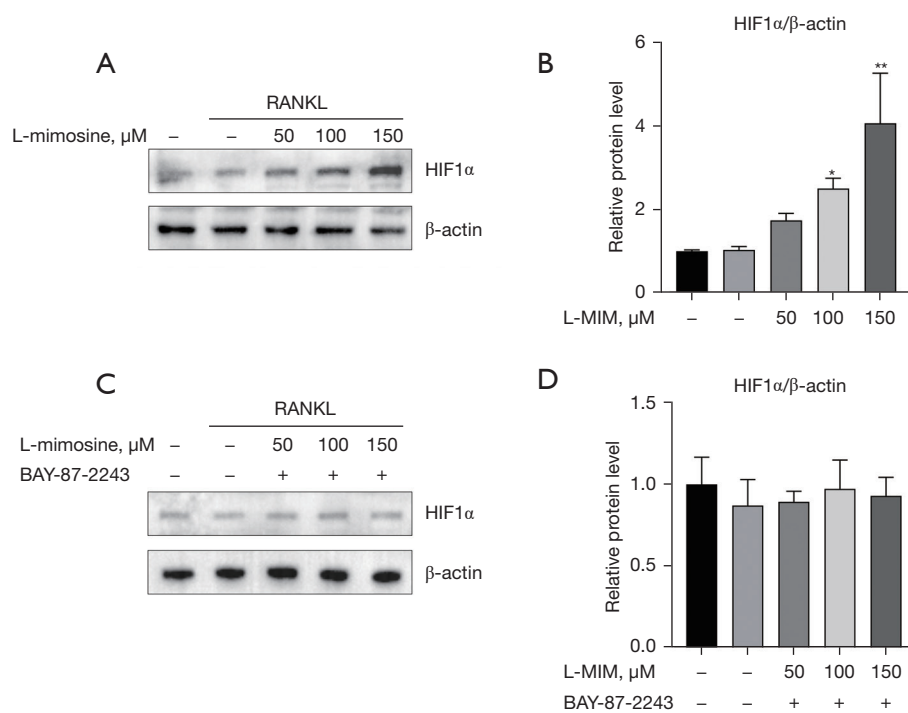


Figure 2 L-mimosine induces HIF1 α expression at the protein level in osteoclast differentiation. (A) The RAW264.7 cells were treated with or without L-mimosine (50, 100, and 150 μ M) for 0.5 h and then treated with 35 ng/mL RANKL for 24 h. Total protein was extracted and subjected to western blot analysis using antibodies against HIF1 α . (C) RANKL-stimulated RAW264.7 cells treated with L-mimosine were added to BAY-87-2243 (10 nM) for 24 h. (B,D) The relative protein expressions were normalized to β -actin and analyzed by ImageJ software. The data are expressed as the mean \pm SD of the 3 independent experiments; *, $P < 0.05$, **, $P < 0.01$ vs. RANKL group. HIF1 α , hypoxia-inducible factor 1 alpha; RANKL, receptor activator of NF- κ B ligand.

increasing the concentration of L-mimosine, elevated the number and morphology of F-actin rings (see *Figure 4A-4C*). Similar to TRAP staining, the enhanced trend of osteoclast differentiation by HIF1 α was attenuated by BAY-87-2243 (see *Figure 5A-5C*).

HIF1 α enhances the RANKL-induced mRNA expression of osteoclast-specific genes

TRAP, cathepsin K, MMP9, and β 3-integrin are osteoclast-specific genes that play essential roles in osteoclast differentiation. To verify the function of HIF1 α in osteoclast differentiation, we examined the effect of L-mimosine-induced HIF1 α expression on the mRNA expression of these genes. The result showed that the mRNA levels of these genes were increased to different degrees compared to the RANKL control group correlated with L-mimosine concentrations (see *Figure 6A-6D*). As expected, the increasing trend in these genes was eliminated by the BAY-

87-2243 treatment (see *Figure 6E-6H*), indicating that HIF1 α has a promoting effect on osteoclast-specific gene expression.

HIF1 α upregulates NFATc1, c-Fos, and c-Jun expression during osteoclast differentiation

As NFATc1, c-Fos and c-Jun are significant transcription factors involved in osteoclast differentiation, we explored whether HIF1 α increased their expression with or without RANKL and L-mimosine using RT-PCR and western blot assays. As *Figure 7* shows, stimulation with L-mimosine enhanced the mRNA (see *Figure 7B-7D*) and protein levels (see *Figure 7A*) of NFATc1, c-Fos, and c-Jun, compared to the group cultured only with RANKL. However, when HIF1 α was inhibited by BAY-87-2243, the mRNA (see *Figure 7I-7K*) and protein levels (see *Figure 7H*) decreased to different degrees. These results confirm the promoting effects of HIF1 α on RANKL-induced NFATc1, c-Fos, and c-Jun expression.

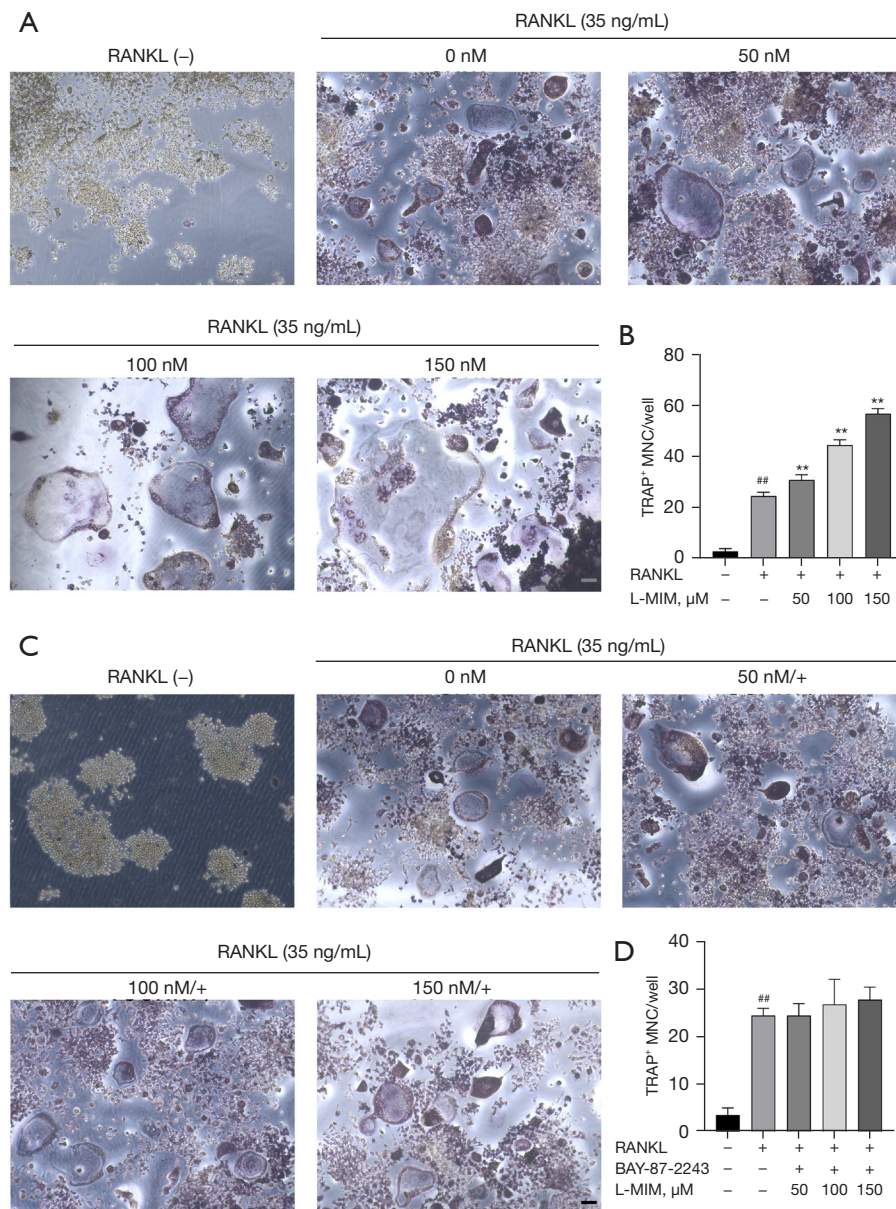


Figure 3 HIF1 α enhances RANKL-induced osteoclast differentiation. (A) RANKL-stimulated RAW264.7 cells were treated for 5 d with or without L-mimosine and (C) additionally treated with BAY-87-2243, and then underwent TRAP staining; representative images are shown (magnification =100 \times). (B,D) TRAP-positive multi-nucleated (nuclei ≥ 3) cells in each treatment group were considered mature osteoclasts. The data are expressed as the mean \pm SD of the 3 independent experiments; ^{##}, $P < 0.01$, *vs.* control group; ^{**}, $P < 0.01$ *vs.* RANKL group. HIF1 α , hypoxia-inducible factor 1 alpha; RANKL, receptor activator of NF- κ B ligand; L-MIM, L-mimosine; TRAP, tartrate-resistant acid phosphatase; SD, standard deviation.

HIF1 α promotes the RANKL-activated MAPK pathway

The MAPK (p38, ERK, and JNK) pathways are involved in numerous cellular processes, such as proliferation, differentiation, motility, apoptosis, and survival. They

are critical pathways involved in RANKL-induced osteoclastogenesis. Thus, to determine whether HIF1 α affects the MAPK pathways during osteoclast differentiation, the protein expression levels of p-p38, p-ERK, and p-JNK were investigated by western blot after 35 ng/mL RANKL

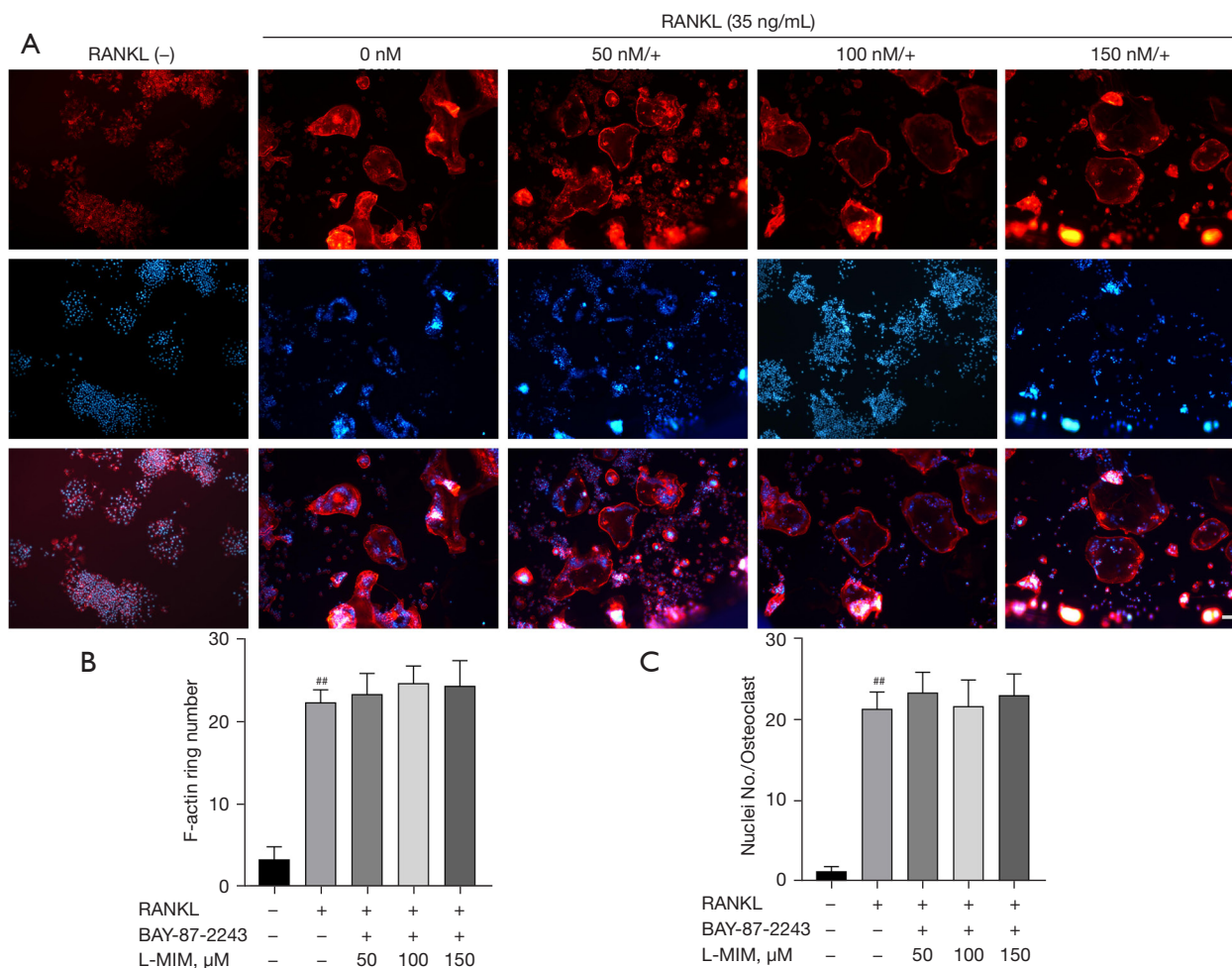


Figure 4 BAY-87-2243 inhibits F-actin ring formation promoted by HIF1 α . (A) RANKL-induced RAW264.7 cells treated with L-mimosine were added to BAY-87-2243. F-actin (red) and nuclei (blue) images were acquired by fluorescence microscope (magnification =100 \times). (B,C) Quantification analyses of F-actin ring size and number of nuclei per osteoclast. The data are expressed as the mean \pm SD of the 3 independent experiments; ^{##}, $P < 0.01$, vs. control group. HIF1 α , hypoxia-inducible factor 1 alpha; RANKL, receptor activator of NF- κ B ligand; L-MIM, L-mimosine; SD, standard deviation.

stimulation with or without L-mimosine (50, 100, and 150 μM). The results indicated that HIF1 α promoted the phosphorylation of MAPKs (p38, ERK, and JNK) in the presence of RANKL (35 ng/mL). As *Figure 8A-8D* show, the phosphorylation of p38, ERK, and JNK relative to total p38, ERK, and JNK were significantly increased by HIF1 α in the RAW264.7 cells. Further, the inhibition of HIF1 α expression by BAY-87-2243 eliminated the increased expression of L-mimosine-induced MAPKs (see *Figure 8E-8H*).

Discussion

As the only multi-nucleated macrophages with bone

resorption capacity *in vivo*, osteoclasts are essential for maintaining normal bone structures (33). Abnormal osteoclast activity often leads to bone loss diseases, such as osteoporosis (34), RA (35), and pathologic fractures (5). A hypoxia microenvironment is a common feature of these diseases (36-38). In recent years, the relationship between osteoclasts and hypoxia has been extensively investigated. HIF1 α acts as a major component of the cellular response to hypoxia; however, the direct effect of HIF1 α on osteoclasts has yet to be fully elucidated. This study demonstrated for the first time that HIF1 α has a direct positive effect on osteoclast differentiation by upregulating the MAPK pathways.

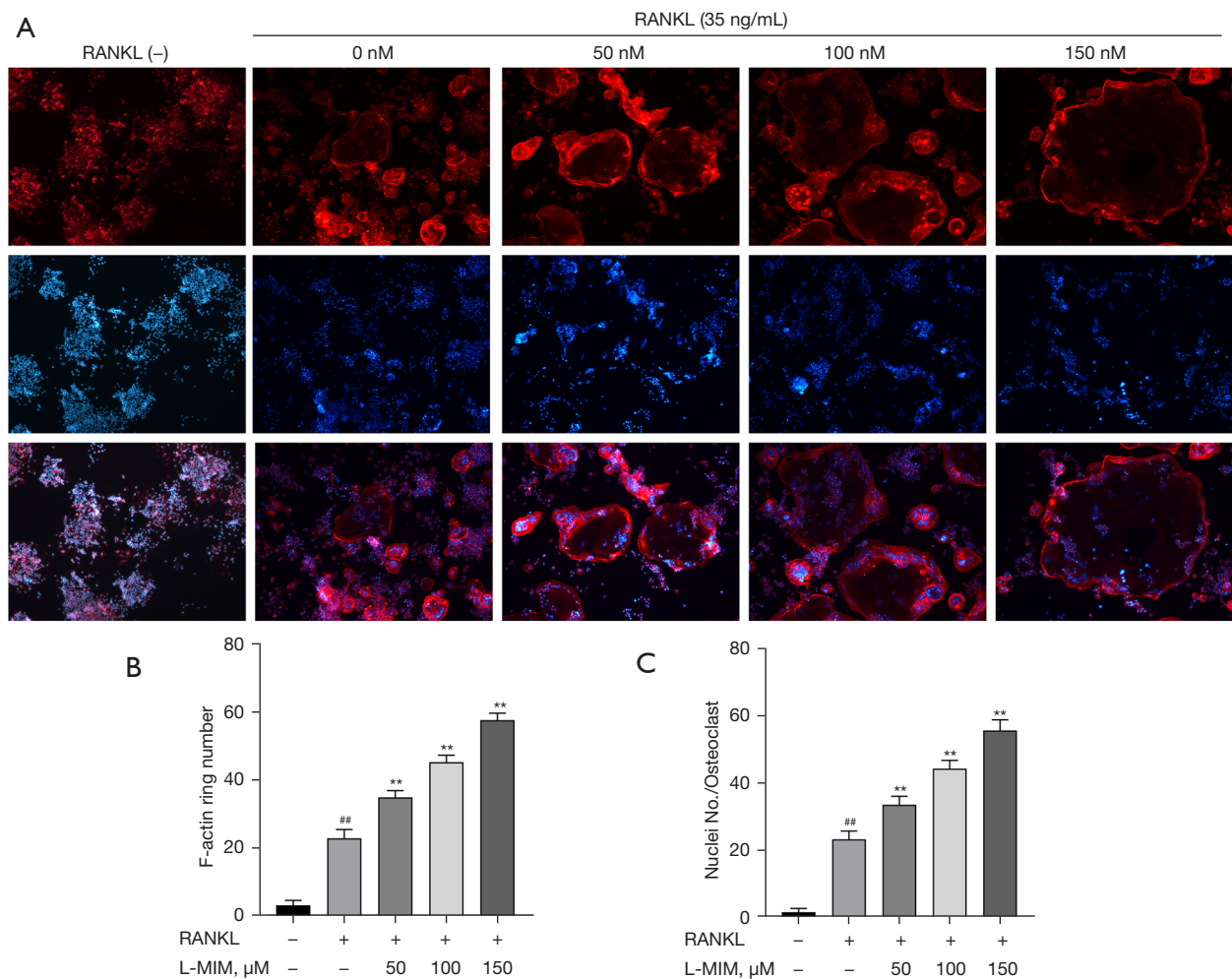


Figure 5 HIF1 α promotes F-actin ring formation. (A) RAW264.7 cells were induced with RANKL with or without L-mimosine (0, 50, 100, and 150 μ M) at the indicated concentrations for 5 d. Images of F-actin (red) and nuclei (blue) were acquired using a fluorescence microscope (magnification, 100 \times). (B,C) Quantification analyses of F-actin ring size and number of nuclei per osteoclast. The data are expressed as the mean \pm SD of the 3 independent experiments; ^{##}, $P < 0.01$, *vs.* control group; ^{**}, $P < 0.01$ *vs.* RANKL group. HIF1 α , hypoxia-inducible factor 1 alpha; RANKL, receptor activator of NF- κ B ligand; L-MIM, L-mimosine; SD, standard deviation.

Stimulation with RANKL differentiates osteoclasts from RAW264.7 cells, and in the absence of RANKL, RAW264.7 cells stabilize proliferation rather than differentiation (39). HIF1 α was activated in osteoclasts using L-mimosine under normoxic conditions. L-mimosine suppressed the activity of PHDs, leading to the stabilization and accumulation of intracellular HIF1 α (40). First, HIF1 α expression was analyzed by western blot. Compared to the untreated cells, HIF1 α expression increased in the L-mimosine-induced cells in a dose-dependent manner. To ensure that HIF1 α was not affected by other factors, the HIF1 α -specific inhibitor, BAY-87-2243, was used with L-mimosine (see Figure 2).

Neither L-mimosine nor BAY-87-2243 cytotoxicity was observed at the experimental concentrations.

To assess the effect of HIF1 α on RANKL-induced osteoclast differentiation from RAW264.7 cells, osteoclast differentiation experiments were performed, and the results indicated that HIF1 α promoted RANKL-induced osteoclast differentiation in a concentration-dependent manner (see Figure 3). A tightly enclosed zone composed of F-actin rings surrounds the bone surface, allowing osteoclasts to secrete hydrogen ions and lytic enzymes into the resorption pit to dissolve the bone (41,42). Thus, as HIF1 α enhances F-actin ring formation, it also partially strengthens osteoclast

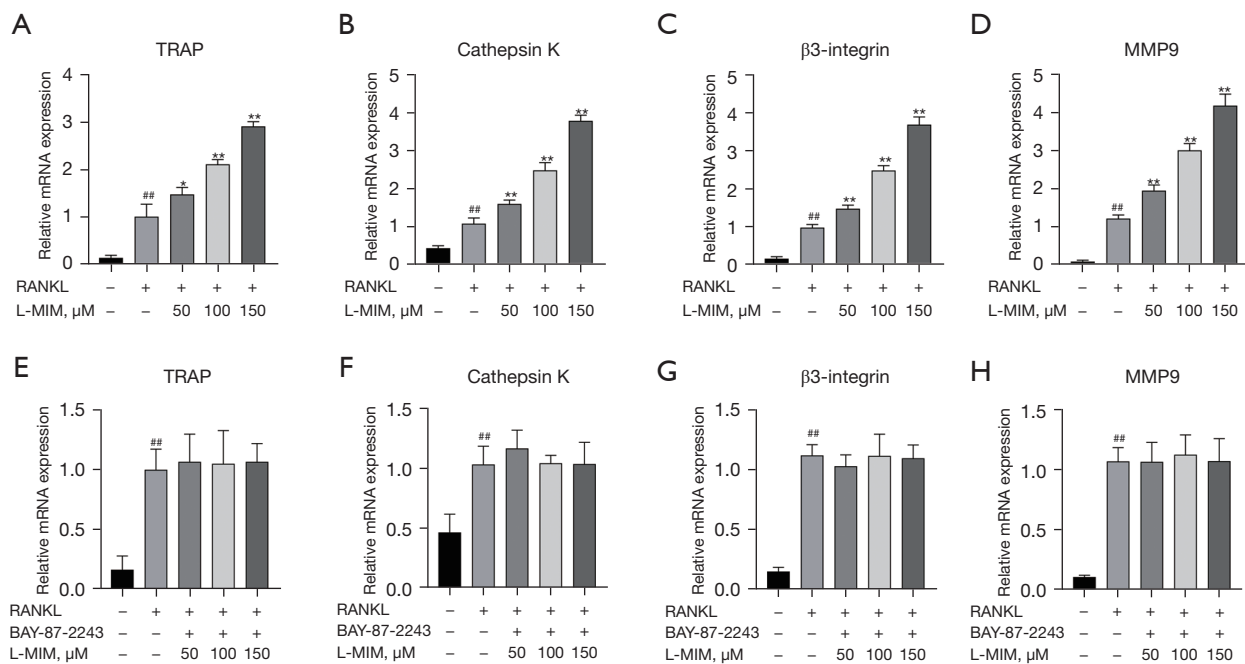


Figure 6 HIF1 α enhances the RANKL-induced mRNA expression of osteoclast-specific genes. The expressed mRNA levels of TRAP (A,E), cathepsin K (B,F), β 3-integrin (C,G), and MMP9 (D,H) were quantitatively measured using qRT-PCR with or without of different concentrations of L-mimosine and BAY-87-2243. The data are expressed as the mean \pm SD of the 3 independent experiments; #, $P < 0.01$, *vs.* control group; *, $P < 0.05$, **, $P < 0.01$ *vs.* RANKL group. HIF1 α , hypoxia-inducible factor 1 alpha; RANKL, receptor activator of NF- κ B ligand; L-MIM, L-mimosine; TRAP, tartrate-resistant acid phosphatase; MMP9, matrix metallo-proteinase 9; qRT-PCR, quantitative real-time polymerase chain reaction; SD, standard deviation.

function (see *Figure 3*). The results of this study were ultimately achieved by promoting the expression levels of osteoclast-specific genes (i.e., TRAP, cathepsin K, MMP9, and β 3-integrin) (see *Figure 6A-6D*). These effects were suppressed by BAY-87-2243.

Previous research has revealed that NFATc1, c-Fos, and c-Jun are the leading factors involved in RANKL-induced osteoclast formation (43-45). Another report indicated that the absence of mice osteoclast-specific gene (NFATc1) impairs osteoclastogenesis and eventually leads to osteoporosis (46). The significance of c-Fos in the early stages of osteoclast formation is remarkable (47). Additionally, c-Fos and c-Jun regulate the NFATc1 promoter region to enhance NFATc1 expression and its downstream transcriptional targets (12,48). In this study, the western blotting and RT-PCR results indicate that HIF1 α positively affects the expression levels of NFATc1, c-Fos, and c-Jun. This positive effect was minimal after the inhibition of HIF1 α expression (see *Figure 7*).

The MAPK (p38, ERK, and JNK) pathways are among the most significant pathways that respond to

stimulation and deliver stimuli from the extracellular space into the nucleus (12). P38 enhances the activity of the microphthalmia-associated transcription factor and TRAP expression to regulate the early stages of osteoclast differentiation (49,50). ERK and JNK are key factors in the proliferation and differentiation of osteoclasts; the phosphorylation of ERK and JNK can induce osteoclast proliferation and differentiation (51). Previous study has shown that the phosphorylation of ERK, JNK, and p38 is significantly increased during RANKL-stimulated macrophage differentiation into osteoclasts (52). The present study showed that HIF1 α increases the phosphorylation of p38, ERK, and JNK in RANKL-induced osteoclasts. After BAY-87-2243 stopped the stimulation of HIF1 α , the phosphorylation levels of p38, ERK and JNK were significantly reduced (see *Figure 8*).

In conclusion, our results demonstrated for the first time that HIF1 α serves as a promoter in RANKL-induced osteoclast differentiation by directly stimulating the osteoclast MAPK signaling pathways. However, while the expression of HIF1 α was increased, the cells were not

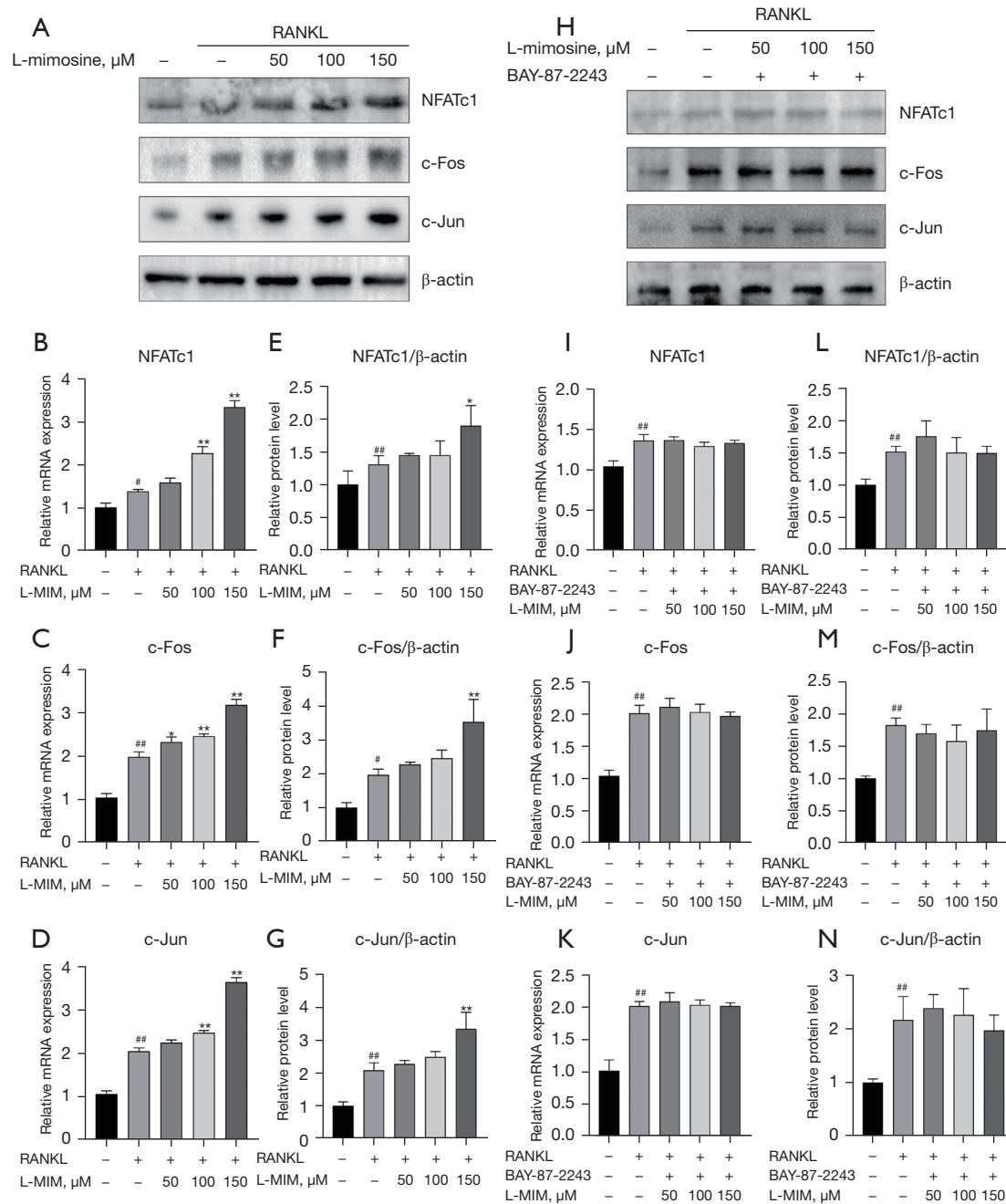


Figure 7 HIF1 α upregulates NFATc1, c-Fos, and c-Jun expression during osteoclast differentiation. (A) RANKL-stimulated RAW264.7 cells were treated with or without different concentrations of L-mimosine (0, 50, 100, and 150 μM). (H) RANKL-induced RAW264.7 cells were treated with both L-mimosine and BAY-87-2243, and proteins, including NFATc1, c-Fos, and c-Jun, were measured using western blotting. (E-G,L-N) The protein expression level was quantitatively analyzed relative to β -actin and calculated using ImageJ software. (B-D,I-K) Quantitative analyses of the relative mRNA expression of osteoclasts specific genes: transcription factors NFATc1, c-Fos, and c-Jun were performed by RT-PCR in the RANKL-induced RAW264.7 cells treated with L-mimosine and L-mimosine + BAY-87-2243. All the data in the figures are presented as the mean \pm SD of the 3 independent experiments; #, $P < 0.05$, ##, $P < 0.01$ vs. control group; *, $P < 0.05$, **, $P < 0.01$ vs. RANKL group. HIF1 α , hypoxia-inducible factor 1 alpha; RANKL, receptor activator of NF- κ B ligand; L-MIM, L-mimosine; RT-PCR, real-time polymerase chain reaction; SD, standard deviation.

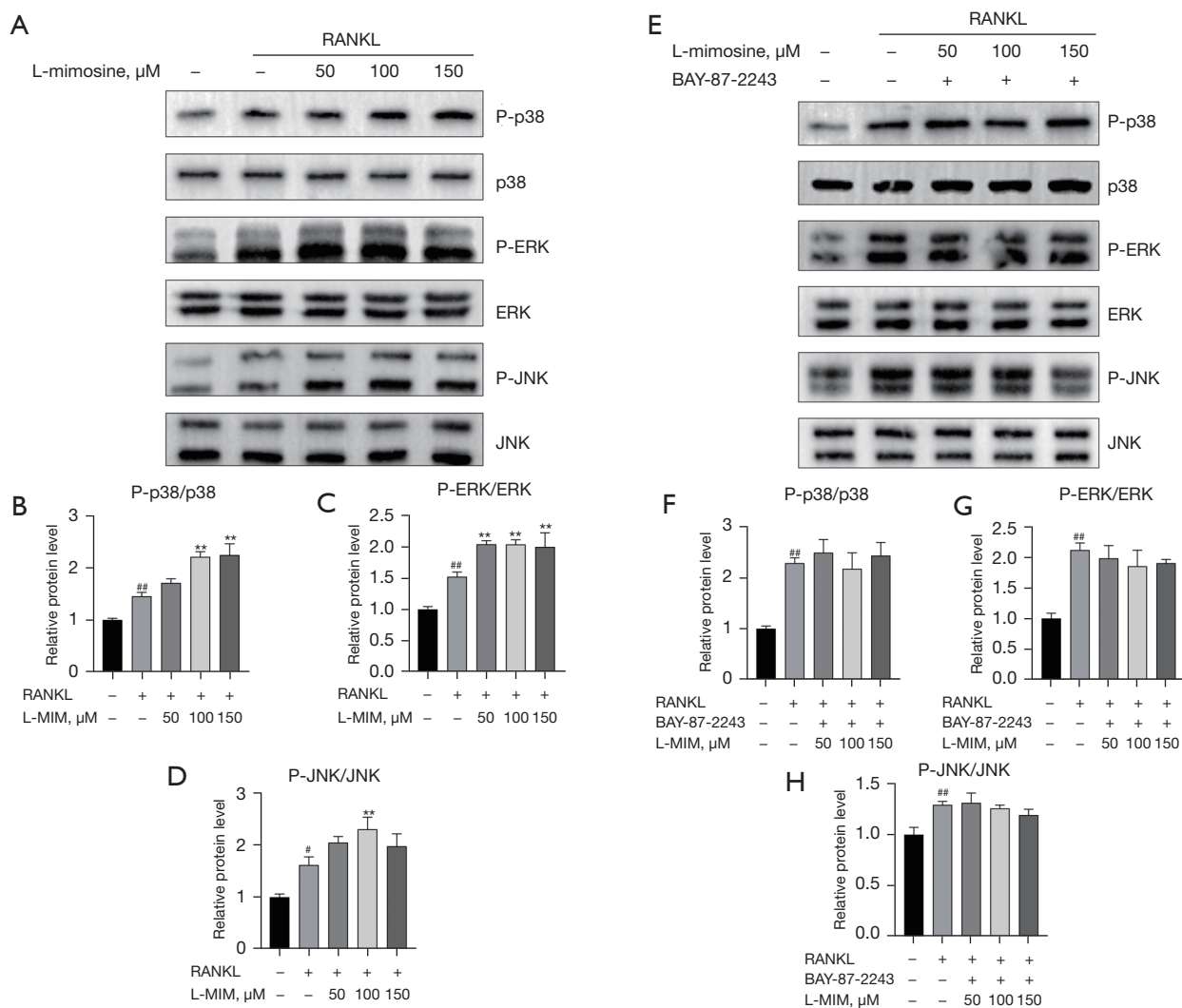


Figure 8 HIF1 α promotes the RANKL-activated MAPK pathway. RAW264.7 cells were pretreated with L-mimosine or both L-mimosine and BAY-87-2243 for 0.5 h, followed by 35 ng/mL of RANKL for the indicated times, and the total proteins were extracted and evaluated by western blot assays for the MAPK (A,E) pathways. The average ratios of phosphor-p38 relative to p38, phosphor-ERK relative to ERK, and phosphor-JNK relative to JNK are shown. The relative intensities of the protein bands (B-D,F-H) were quantified by ImageJ software. The data are expressed as the mean \pm SD of the 3 independent experiments; #, $P < 0.05$, ##, $P < 0.01$, vs. control group; **, $P < 0.01$ vs. RANKL group. HIF1 α , hypoxia-inducible factor 1 alpha; RANKL, receptor activator of NF- κ B ligand; L-MIM, L-mimosine; MAPK, mitogen-activated protein kinase; ERK, extracellular signal-regulated kinase; JNK, Jun N-terminal kinase; SD, standard deviation.

in a real state of hypoxia and nutrient deficiency, and the mimicking of *in vitro* invariant hypoxia did not truly reflect the changing hypoxic environment under physiological or pathological conditions *in vivo* (53). Additionally, different degrees and durations of low-oxygen environments have diverse effects on osteoclasts (54). Overall, this study revealed that hypoxia is a common feature of bone loss diseases, such as osteoporosis, pathologic bone fractures,

and RA. Our findings may provide novel ideas and directions for subsequent research and the treatment of bone loss diseases.

Acknowledgments

Funding: This study was supported by grants from the Key Project of Natural Science Basic Research Plan of Shaanxi

Province (No. 2022JZ-43) and the National Science Foundation of China (No. 82070909).

Footnote

Reporting Checklist: The authors have completed the MDAR reporting checklist. Available at <https://atm.amegroups.com/article/view/10.21037/atm-22-4603/rc>

Data Sharing Statement: Available at <https://atm.amegroups.com/article/view/10.21037/atm-22-4603/dss>

Conflicts of Interest: All authors have completed the ICMJE uniform disclosure form (available at <https://atm.amegroups.com/article/view/10.21037/atm-22-4603/coif>). The authors have no conflicts of interest to declare.

Ethical Statement: The authors are accountable for all aspects of the work in ensuring that questions related to the accuracy or integrity of any part of the work are appropriately investigated and resolved.

Open Access Statement: This is an Open Access article distributed in accordance with the Creative Commons Attribution-NonCommercial-NoDerivs 4.0 International License (CC BY-NC-ND 4.0), which permits the non-commercial replication and distribution of the article with the strict proviso that no changes or edits are made and the original work is properly cited (including links to both the formal publication through the relevant DOI and the license). See: <https://creativecommons.org/licenses/by-nc-nd/4.0/>.

References

- Boyle WJ, Simonet WS, Lacey DL. Osteoclast differentiation and activation. *Nature* 2003;423:337-42.
- Datta HK, Ng WF, Walker JA, et al. The cell biology of bone metabolism. *J Clin Pathol* 2008;61:577-87.
- Teitelbaum SL. Osteoclasts: what do they do and how do they do it? *Am J Pathol* 2007;170:427-35.
- Kobayashi S, Takahashi HE, Ito A, et al. Trabecular minimodeling in human iliac bone. *Bone* 2003;32:163-9.
- Abe T, Shin J, Hosur K, et al. Regulation of osteoclast homeostasis and inflammatory bone loss by MFG-E8. *J Immunol* 2014;193:1383-91.
- Knowles HJ. Hypoxic regulation of osteoclast differentiation and bone resorption activity. *Hypoxia (Auckl)* 2015;3:73-82.
- Boyce BF, Xing L. Functions of RANKL/RANK/OPG in bone modeling and remodeling. *Arch Biochem Biophys* 2008;473:139-46.
- Song C, Yang X, Lei Y, et al. Evaluation of efficacy on RANKL induced osteoclast from RAW264.7 cells. *J Cell Physiol* 2019;234:11969-75.
- Kobayashi N, Kadono Y, Naito A, et al. Segregation of TRAF6-mediated signaling pathways clarifies its role in osteoclastogenesis. *EMBO J* 2001;20:1271-80.
- Asagiri M, Takayanagi H. The molecular understanding of osteoclast differentiation. *Bone* 2007;40:251-64.
- Walsh MC, Kim N, Kadono Y, et al. Osteoimmunology: interplay between the immune system and bone metabolism. *Annu Rev Immunol* 2006;24:33-63.
- Matsuo K, Galson DL, Zhao C, et al. Nuclear factor of activated T-cells (NFAT) rescues osteoclastogenesis in precursors lacking c-Fos. *J Biol Chem* 2004;279:26475-80.
- Wagner EF, Eferl R. Fos/AP-1 proteins in bone and the immune system. *Immunol Rev* 2005;208:126-40.
- Takayanagi H. Osteoimmunology: shared mechanisms and crosstalk between the immune and bone systems. *Nat Rev Immunol* 2007;7:292-304.
- Lee SE, Woo KM, Kim SY, et al. The phosphatidylinositol 3-kinase, p38, and extracellular signal-regulated kinase pathways are involved in osteoclast differentiation. *Bone* 2002;30:71-7.
- Zhao Q, Wang X, Liu Y, et al. NFATc1: functions in osteoclasts. *Int J Biochem Cell Biol* 2010;42:576-9.
- Negishi-Koga T, Takayanagi H. Ca²⁺-NFATc1 signaling is an essential axis of osteoclast differentiation. *Immunol Rev* 2009;231:241-56.
- Wang GL, Jiang BH, Rue EA, et al. Hypoxia-inducible factor 1 is a basic-helix-loop-helix-PAS heterodimer regulated by cellular O₂ tension. *Proc Natl Acad Sci U S A* 1995;92:5510-4.
- Wang Y, Wan C, Deng L, et al. The hypoxia-inducible factor alpha pathway couples angiogenesis to osteogenesis during skeletal development. *J Clin Invest* 2007;117:1616-26.
- Arnett TR, Gibbons DC, Utting JC, et al. Hypoxia is a major stimulator of osteoclast formation and bone resorption. *J Cell Physiol* 2003;196:2-8.
- Zhu J, Tang Y, Wu Q, et al. HIF-1 α facilitates osteocyte-mediated osteoclastogenesis by activating JAK2/STAT3 pathway in vitro. *J Cell Physiol* 2019;234:21182-92.
- Hulley PA, Bishop T, Vernet A, et al. Hypoxia-inducible factor 1-alpha does not regulate osteoclastogenesis but enhances bone resorption activity via prolyl-4-hydroxylase

2. *J Pathol* 2017;242:322-33.
23. Chaudhary P, Babu GS, Sobti RC, et al. HGF regulate HTR-8/SVneo trophoblastic cells migration/invasion under hypoxic conditions through increased HIF-1 α expression via MAPK and PI3K pathways. *J Cell Commun Signal* 2019;13:503-21.
 24. Itsuji T, Tonomura H, Ishibashi H, et al. Hepatocyte growth factor regulates HIF-1 α -induced nucleus pulposus cell proliferation through MAPK-, PI3K/Akt-, and STAT3-mediated signaling. *J Orthop Res* 2021;39:1184-91.
 25. Zhou W, Zhou W, Zeng Q, et al. MicroRNA-138 inhibits hypoxia-induced proliferation of endothelial progenitor cells via inhibition of HIF-1 α -mediated MAPK and AKT signaling. *Exp Ther Med* 2021;22:996.
 26. Kaur B, Khwaja FW, Severson EA, et al. Hypoxia and the hypoxia-inducible-factor pathway in glioma growth and angiogenesis. *Neuro Oncol* 2005;7:134-53.
 27. Lee JW, Bae SH, Jeong JW, et al. Hypoxia-inducible factor (HIF-1) α : its protein stability and biological functions. *Exp Mol Med* 2004;36:1-12.
 28. Aranha AM, Zhang Z, Neiva KG, et al. Hypoxia enhances the angiogenic potential of human dental pulp cells. *J Endod* 2010;36:1633-7.
 29. Dengler VL, Galbraith M, Espinosa JM. Transcriptional regulation by hypoxia inducible factors. *Crit Rev Biochem Mol Biol* 2014;49:1-15.
 30. Asikainen TM, White CW. HIF stabilizing agents: shotgun or scalpel? *Am J Physiol Lung Cell Mol Physiol* 2007;293:L555-6.
 31. Warnecke C, Griethe W, Weidemann A, et al. Activation of the hypoxia-inducible factor-pathway and stimulation of angiogenesis by application of prolyl hydroxylase inhibitors. *FASEB J* 2003;17:1186-8.
 32. Du J, Wang C, Chen Y, et al. Targeted downregulation of HIF-1 α for restraining circulating tumor microemboli mediated metastasis. *J Control Release* 2022;343:457-68.
 33. Chambers TJ. Regulation of the differentiation and function of osteoclasts. *J Pathol* 2000;192:4-13.
 34. Mazziotti G, Angeli A, Bilezikian JP, et al. Glucocorticoid-induced osteoporosis: an update. *Trends Endocrinol Metab* 2006;17:144-9.
 35. McHugh KP, Shen Z, Crotti TN, et al. The role of cell-substrate interaction in regulating osteoclast activation: potential implications in targeting bone loss in rheumatoid arthritis. *Ann Rheum Dis* 2010;69 Suppl 1:i83-85.
 36. Choi S, You S, Kim D, et al. Transcription factor NFAT5 promotes macrophage survival in rheumatoid arthritis. *J Clin Invest* 2017;127:954-69.
 37. Miyauchi Y, Sato Y, Kobayashi T, et al. HIF1 α is required for osteoclast activation by estrogen deficiency in postmenopausal osteoporosis. *Proc Natl Acad Sci U S A* 2013;110:16568-73.
 38. Pountos I, Panteli M, Panagiotopoulos E, et al. Can we enhance fracture vascularity: What is the evidence? *Injury* 2014;45 Suppl 2:S49-57.
 39. Kong L, Smith W, Hao D. Overview of RAW264.7 for osteoclastogenesis study: Phenotype and stimuli. *J Cell Mol Med* 2019;23:3077-87.
 40. Janjić K, Bauer P, Edelmayer M, et al. Angiogenin production in response to hypoxia and l-mimosine in periodontal fibroblasts. *J Periodontol* 2019;90:674-81.
 41. Jiang C, Shang J, Li Z, et al. Lanthanum Chloride Attenuates Osteoclast Formation and Function Via the Downregulation of Rankl-Induced Nf- κ b and Nfatc1 Activities. *J Cell Physiol* 2016;231:142-51.
 42. Kong L, Ma R, Cao Y, et al. Cell cytoskeleton and proliferation study for the RANKL-induced RAW264.7 differentiation. *J Cell Mol Med* 2021;25:4649-57.
 43. Ikeda F, Nishimura R, Matsubara T, et al. Critical roles of c-Jun signaling in regulation of NFAT family and RANKL-regulated osteoclast differentiation. *J Clin Invest* 2004;114:475-84.
 44. Koga T, Matsui Y, Asagiri M, et al. NFAT and Osterix cooperatively regulate bone formation. *Nat Med* 2005;11:880-5.
 45. Zhang Q, Tang X, Liu Z, et al. Hesperetin Prevents Bone Resorption by Inhibiting RANKL-Induced Osteoclastogenesis and Jnk Mediated Irf-3/c-Jun Activation. *Front Pharmacol* 2018;9:1028.
 46. Kim JH, Kim N. Regulation of NFATc1 in Osteoclast Differentiation. *J Bone Metab* 2014;21:233-41.
 47. Grigoriadis AE, Wang ZQ, Cecchini MG, et al. c-Fos: a key regulator of osteoclast-macrophage lineage determination and bone remodeling. *Science* 1994;266:443-8.
 48. Boyce BF, Xiu Y, Li J, et al. NF- κ B-Mediated Regulation of Osteoclastogenesis. *Endocrinol Metab (Seoul)* 2015;30:35-44.
 49. Cong Q, Jia H, Li P, et al. p38 α MAPK regulates proliferation and differentiation of osteoclast progenitors and bone remodeling in an aging-dependent manner. *Sci Rep* 2017;7:45964.
 50. Matsumoto M, Sudo T, Saito T, et al. Involvement of p38 mitogen-activated protein kinase signaling pathway in osteoclastogenesis mediated by receptor activator of NF- κ B ligand (RANKL). *J Biol Chem* 2000;275:31155-61.

51. Yang X, Liang J, Wang Z, et al. Sesamol Protects Mice From Ovariectomized Bone Loss by Inhibiting Osteoclastogenesis and RANKL-Mediated NF- κ B and MAPK Signaling Pathways. *Front Pharmacol* 2021;12:664697.
52. Zhou F, Mei J, Yuan K, et al. Isorhamnetin attenuates osteoarthritis by inhibiting osteoclastogenesis and protecting chondrocytes through modulating reactive oxygen species homeostasis. *J Cell Mol Med* 2019;23:4395-407.
53. Lu C, Saless N, Wang X, et al. The role of oxygen during fracture healing. *Bone* 2013;52:220-9.
54. Knowles HJ, Athanasou NA. Acute hypoxia and osteoclast activity: a balance between enhanced resorption and increased apoptosis. *J Pathol* 2009;218:256-64.

Cite this article as: Wang D, Liu L, Qu Z, Zhang B, Gao X, Huang W, Feng M, Gong Y, Kong L, Wang Y, Yan L. Hypoxia-inducible factor 1 α enhances RANKL-induced osteoclast differentiation by upregulating the MAPK pathway. *Ann Transl Med* 2022;10(22):1227. doi: 10.21037/atm-22-4603